CrossMark

Trends in black carbon and size-resolved particle number concentrations and vehicle emission factors under real-world conditions

Patricia Krecl [a, *], Christer Johansson [b, c], Admir Créso Targino [a], Johan Ström [b], Lars Burman [c]

[a] Graduate Program in Environmental Engineering, Federal University of Technology, Av. Pioneiros 3131, 86036-370 Londrina, PR, Brazil
[b] Department of Environmental Science and Analytical Chemistry, Stockholm University, Svante Arrhenius väg 8, SE-11418 Stockholm, Sweden
[c] Stockholm Environment and Health Administration, Fleminggatan 4, SE-10420 Stockholm, Sweden

HIGHLIGHTS

- Traffic-related pollutants were measured within a street canyon in 2006 and 2013.
- Emission factors (EF) were calculated from these measurements for both years.
- Large reduction in black carbon (BC) and particle number (PN) concentrations.
- EF are consistent with on-road studies but higher than simulated by emission models.
- Traffic emissions largely decreased for BC (61%), but less for PN (34%).

ARTICLE INFO

ABSTRACT

Kerbside concentrations of NOx, black carbon (BC), total number of particles (diameter > 4 nm) and number size distribution (28—410 nm) were measured at a busy street canyon in Stockholm in 2006 and 2013. Over this period, there was an important change in the vehicle fleet due to a strong dieselisation process of light-duty vehicles and technological improvement of vehicle engines. This study assesses the impact of these changes on ambient concentrations and particle emission factors (EF). EF were calculated by using a novel approach which combines the NOx tracer method with positive matrix factorisation (PMF) applied to particle number size distributions. NOx concentrations remained rather constant between these two years, whereas a large decrease in particle concentrations was observed, being on average 60% for BC, 50% for total particle number, and 53% for particles in the range 28—100 nm. The PMF analysis yielded three factors that were identified as contributions from gasoline vehicles, diesel fleet, and urban background. This separation allowed the calculation of the average vehicle EF for each particle metric per fuel type. In general, gasoline EF were lower than diesel EF, and EF for 2013 were lower than the ones derived for 2006. The EF_BC decreased 77% for both gasoline and diesel fleets, whereas the particle number EF reduction was higher for the gasoline (79%) than for the diesel (37%) fleet. Our EF are consistent with results from other on-road studies, which reinforces that the proposed methodology is suitable for EF determination and to assess the effectiveness of policies implemented to reduce vehicle exhaust emissions. However, our EF are much higher than EF simulated with traffic emission models (HBEFA and COPERT) that are based on dynamometer measurements, except for EF_BC for diesel vehicles. This finding suggests that the EF from the two leading models in Europe should be revised for BC (gasoline vehicles) and particle number (all vehicles), since they are used to compile national inventories for the road transportation sector and also to assess their associated health effects. Using the calculated kerbside EF, we estimated that the traffic emissions were lower in 2013 compared to 2006 with a 61% reduction for BC (due to decreases in both gasoline and diesel emissions), and 34—45% for particle number (reduction only in gasoline emissions). Limitations of the application of these EF to other studies are also discussed.

* Corresponding author.
E-mail address: patriciak@utfpr.edu.br (P. Krecl).

1. Introduction

The World Health Organization (WHO) has recently recognised that ambient particulate pollution is a public health emergency accounting for about 3.0 million premature deaths annually (WHO, 2016). The WHO assessment was based on monitored particulate matter (PM) mass concentrations from 3000 urban areas around the world and complemented by modelled data in areas where measurements are scarce. PM is a complex mixture of organic and inorganic substances such as sulphates, nitrates, ammonium, sodium chloride, black carbon (BC), mineral dust and water (Fuzzi et al., 2015) and is usually regulated by mass with no chemical speciation. However, the predominance of certain toxic substances is size-dependent and hence when PM is treated as a bulk, the specific constituents responsible for acute health outcomes may not be pinpointed. This way, there has been a consensus within the scientific community to quantify the species within the PM that are most harmful to human health to streamline strategies to abate noncommunicable diseases (e.g., Rohr and Wyzga, 2012; Chung et al., 2015).

BC and ultrafine particles (UFP, diameter D_p < 100 nm) are specific constituents of PM, but despite their well-established impacts on human health (Shah et al., 2008; Janssen et al., 2012; HEI, 2013; Maher et al., 2016), they are not regulated in national air quality standards (NAQS). As a result, they are not well characterised yet. BC particles —emitted from the combustion of any carbonaceous fuel— strongly absorb electromagnetic radiation both in the visible and infrared spectra, thus contributing to global warming (Bond et al., 2013). They make up a substantial fraction of ultrafine carbonaceous particles and Krecl et al. (2015) found correlations above 80% between BC and particle number (PN) concentrations in the size range 60–100 nm at a kerbside site in Stockholm. Urban UFP are products of combustion and secondary atmospheric processes, with on-road traffic contributing up to 90% of the total UFP in polluted roadside environments (Kumar et al., 2014), especially in street canyons where natural ventilation is frequently reduced (e.g., Imhof et al., 2005; Wang et al., 2010; Krecl et al., 2016). Because UFP are too small to accumulate aerosol mass, their concentration is better evaluated by number.

Emissions from vehicles are usually estimated by multiplying EF —defined as the average rate of emission of a pollutant per km driven or fuel consumed (Franco et al., 2013)— by activity rates for a given vehicle category. Accurate and updated knowledge of EF for different vehicle categories is crucial to prepare reliable emission inventories which, in turn, are strategic tools for air quality management, since they: i) help identify the major emitters and prioritising sectors for emission reduction, ii) provide spatially and temporally allocated emissions that are input data for atmospheric dispersion models, iii) can be used for setting off future air quality targets, iv) aid in the monitoring of the effectiveness of policy intervention to control vehicle emissions by using trends in emission inventory data, and v) help assess the health impacts of different sources of exposure.

The European Union (EU) implements both NAQS and emission mitigation controls to manage the air quality, and state members are required to annually report emissions of several criteria air pollutants (NOx, CO, NMVOC, SO_2, NH_3, TSP, PM_{10} and $PM_{2.5}$, heavy metals, dioxins and PAH) for different end-use sectors following specific guidelines (EMEP, 2013). In 2013, the road-transport sector was still the largest contributor to NOx emissions (46%), and accounted for 13% and 15% of the total PM_{10} and $PM_{2.5}$ primary emissions, respectively (EEA, 2015a). EU parties to the Convention on Long-Range Transboundary Air Pollution (CLRTAP) revised Gothenburg Protocol are encouraged to voluntary report BC

emissions, with EF_{BC} calculated as a fraction of estimated emissions of $PM_{2.5}$. However, only 17 of 28 countries reported BC emissions for the year 2013 (EEA, 2015b).

The EF for on-road vehicles can be derived from emission models and require input data of different complexity (Smit et al., 2010) or are derived from emission measurements conducted under controlled (dynamometer testing) or real-world conditions (tunnel studies, vehicle chase, road-side and on-board measurements) (Franco et al., 2013). Results of dynamometer tests are commonly used for approval of road vehicles and engines but, since they are not able to capture the full range of real-world patterns, they should be always validated with real-world measurements. A recent example of the importance of this validation is the outcome of the so called "Dieselgate scandal", which revealed that on-road NOx emissions from diesel passenger cars manufactured by several carmakers are much higher than the laboratory tests (Transport and Environment, 2016).

Depending on the measurement approach, EF can be calculated for single vehicles, vehicle categories, fuel-based categories, or the entire fleet. As highlighted by Franco et al. (2013), the EF for a given pollutant depends on the vehicle characteristics (e.g., engine type, exhaust after-treatment system, maintenance status), fuel specifications, and ambient and operating conditions (air temperature, topography, driving behaviour, traffic situations, among others). Because EF measurements are conducted mainly for pollutants with regulated emissions, data on EF_{BC} and EF_{PN} are very scarce and contain large uncertainties. To reduce the impact of the road transport sector on the environment, a variety of measures has been implemented throughout the world. For example, the EU introduced increasingly strict vehicle emission standards (i.e., Euro standards) for new vehicles to improve air quality, and promoted the dieselisation of the fleet to cut down greenhouse gases emissions because diesel cars have lower CO_2 emissions and lower fuel consumption than gasoline-fuelled engines (Cames and Helmers, 2013).

This study investigates the ambient concentrations and EF trends of BC and PN under real-world conditions within a street canyon in Stockholm (Sweden) in the years 2006 and 2013. Our novel approach for calculating EF combines the tracer method with positive matrix factorisation (PMF) applied to particle number size distribution (PNSD) measurements. This approach differentiates gasoline from diesel contribution, and excludes the background contribution from the street canyon levels. We also discuss the trends in relation to the strong dieselisation process observed in Sweden over the last decade, advances in vehicle technology, and more stringent emission regulations.

2. Material and methods

2.1. Experimental set-up

The sampling campaigns were conducted in a regular (height-to-width ratio of 1) street canyon on Hornsgatan road in the inner city of Stockholm. The traffic on that road transect is organised in four lanes (two lanes in each direction) and controlled by a traffic light situated 67 m from the site. This location was selected because of its high traffic rate (TR), relatively low vehicle speed (VS), and well characterised traffic and vehicle fleet (Burman and Johansson, 2010; Krecl et al., 2015). NOx, BC and total and size-segregated PN concentrations were analysed for two periods in the springs of 2006 and 2013 (11 April - 20 June) when data coverage was maximum for all variables. Concurrent NOx and BC data were collected at an urban background site (Torkel, located 450 m southeast of Hornsgatan site, at 25 m height) to help identify the

PMF factors (Krecl et al., 2015). Both sites are managed by the Stockholm Environment and Health Administration and a complete description of the stations can be found elsewhere (Krecl et al., 2011, 2015).

NOx was monitored with a commercial chemiluminescence analyser model AC31M (Environment SA, France) in both years. In spring 2006, BC was measured with a custom-built Particle Soot Absorption Photometer (c-PSAP, details in Krecl et al., 2011) whereas measurements in 2013 were conducted with a multi-wavelength aethalometer model AE31 (Magee Scientific, USA). These optical filter-based instruments rely on the light-absorbing properties of the carbonaceous aerosols and several post-processing corrections must be applied to eliminate instrumental artifacts, such as filter scattering, particle scattering and loading effects. The c-PSAP and AE31 data were corrected for the loading effect using the methods by Bond et al. (1999) and Virkkula et al. (2007), respectively. As to the scattering corrections, we only accounted for the filter-scattering correction since concurrent measurements of the particle scattering coefficient were not available. Instead, we used data from an intercomparison study conducted at Torkel site in which the c-PSAP (wavelength λ of 525 nm), the AE31 (λ of 660 nm) and a Multiple-Angle Absorption Photometer (MAAP, λ of 670 nm) were collocated during 400 h. The MAAP instrument measures light transmission and scattering to derive BC concentrations and treats particle scattering artifacts using built-in algorithms (Petzold et al., 2002), showing very good agreement with other filter (e.g., Drinovec et al., 2015; Segura et al., 2014) and non-filter based measurements (e.g., Petzold et al., 2005). Hence, linear regression equations were extracted using the MAAP measurements as reference, yielding excellent agreement (R > 0.95) with negligible y-intercept and slopes of 1.028 for the c-PSAP and 1.058 for the AE31. Another advantage with this approach is that the MAAP data used a mass specific attenuation cross section ($\sigma = 7.49 \, m^2 \, g^{-1}$) determined in situ by concurrent 12-h elemental carbon (EC) measurements analysed with the Thermal/Optical Carbon Aerosol Analyser (Sunset Laboratory Inc., USA) and following the NIOSH protocol. Thus, the BC measurements conducted in 2006 and 2013 were both harmonised by using their respective slopes found in the intercomparison study with the MAAP.

Total PN concentrations were measured with condensation particle counters (CPC) with a 50% lower cut-off size at 7 nm (N_7) in 2006 (TSI, model 3022, USA), and at 4 nm (N_4) in 2013 (TSI, model 3775, USA). The PN observations were harmonised using an extensive intercomparison between the two instruments at Hornsgatan site and showed excellent linear correlation (R = 1). Thus, the hourly N_7 data measured in 2006 were adjusted using the CPC 3775 as a reference ($N_{7,adj} = 1.1316 \times N_7 + 1779.6$). Hereafter the adjusted N_7 concentrations for 2006 will be referred to as N_4.

PNSD were recorded with differential mobility particle sizers (DMPS) built at the Department of Applied Environmental Sciences (ITM) and consisted of a bipolar diffusion charger, a custom-built differential mobility analyser (DMA) and a CPC. In 2006, the particle sizer was set up with a Hauke medium-type DMA along with a TSI 3760 CPC (50% lower cut-off at 11 nm) covering the size ranges 28–539 nm (bin middle), operated at 1.5 l min^{-1} aerosol flow rate and 5 l min^{-1} sheath air flow rate (Krecl et al., 2008). In 2013, the DMPS consisted of a Hauke short-type DMA and a TSI CPC 3010 (50% lower cut-off at 10 nm) observing PNSD in the interval 10–410 nm, and was operated at 1.0 l min^{-1} aerosol flow rate and 5 l min^{-1} sheath air flow rate (Tunved et al., 2004). The raw particle electrical mobility distributions were processed by an inversion algorithm with a triangular ideal transfer function, and multiple charge corrections were applied following Wiedensohler (1988). Since the DMPS channels did not match for the whole particle

diameter size range, we used the PN concentrations in the interval 28–453 nm in 2006 and 28–410 nm in 2013. We consider this is a reasonable approach since the number of particles with D_p between 410 and 453 nm is negligible within a busy street where road traffic contributes up to 90% to the UFP concentrations (Kumar et al., 2014 and references therein). Hereafter the integrated PN concentrations in the coincident interval will be referred to as N_{28}. These two DMPS systems were not directly intercompared in this study. However, Wiedensholer et al. (2012) showed that PNSD measured with several custom-built DMPS of similar design as the ones used here were within an uncertainty range of ±10% in the particle range 20–200 nm, and up to 30% for larger particles. In this study, the larger uncertainty for D_p > 200 nm has a reduced effect on our calculations since they make up a very small fraction (3% of N_{28}).

Traffic data (TR and VS) were recorded on Hornsgatan street using an automatic Marksman loop counter, model 660 (Golden River Traffic Ltd., UK). Meteorological measurements were conducted at Torkel rooftop site, including air temperature (T), relative humidity (RH), wind speed (WS), wind direction (WD), precipitation and solar irradiance (details in Krecl et al., 2011).

All data were inspected for anomalous values, and negative and obvious outliers were removed. Integrated DMPS data higher than simultaneous CPC concentrations were also discarded. The remaining data were averaged in 1-h intervals and reported in local standard time (UTC + 1) and in the 24-h notation. An exceptional long-range transport event occurred in the period 24 April - 9 May 2006 (Targino et al., 2013) and was excluded from our analysis to focus on typical pollution conditions in the street canyon.

2.2. Calculation of emission factors

2.2.1. Method

Different techniques have been developed to determine vehicle EF under real-world conditions (Franco et al., 2013), such as remote sensing next to the roads, vehicle chasing, portable emission measurement systems (PEMS), and the so-called tracer method (Imhof et al., 2005; Kumar et al., 2011 and references therein) used in this work. The main advantages of the tracer method are the use of already available community fixed data, and the determination of EF in dense traffic situations with multiple lanes where other techniques fail (vehicle chasing and remote sensing). The inherent drawback, however, is the determination of average EF for the entire fleet (or by vehicle category) driving on that street transect instead of single vehicle EF as measured by chasing and PEMS techniques.

The tracer method has the following characteristics:

i. It uses roadside measurements of air pollutants and links them with local traffic emissions by excluding contributions from other sources impacting the road concentrations. Within street canyons, the local traffic contribution is generally isolated by subtracting concentrations measured at nearby urban background sites from concurrent roadside levels, and assuming that long-range transported compounds equally impact roadside and background pollution (e.g., Wang et al., 2010).

ii. It is suitable for pollutants when dilution is faster than other transformation processes in the frame between the tailpipe and the sampling point. In a street canyon, with a mixing timescale in the order of seconds up to a few minutes, dilution is the absolute dominating transformation for NOx, BC and PN concentrations (Ketzel and Berkowicz, 2004; Pohjola et al., 2003; Zhang et al., 2004).

iii. Then, the vehicle EF of pollutant i (EF$_i$) can be expressed as:

$$EF_i = \frac{C_i}{TR} \, D, \tag{1}$$

where C_i is the concentration of pollutant i due to emissions of vehicles driving on that street, TR is the traffic rate on that street, and D is the dilution rate.

    iv. Finally, the dilution rate is calculated from the measured pollutants assuming that the particles and gases of interest are diluted in the same way as an inert tracer with known EF. NOx has been proven a very good tracer at street level (Imhof et al., 2005; Wang et al., 2010), presents a high correlation with other traffic-related pollutants such as BC and PN concentrations (e.g., Krecl et al., 2015), and its emissions are relatively well-known for a variety of traffic situations and are available from several on-road traffic emission databases.

In this study, a new approach was used to isolate the local traffic contribution from other possible sources. PMF was applied onto hourly PNSD from 28 to 410 nm measured at the canyon site and three factors were identified, separating the local contribution of traffic (split into gasoline and diesel fleets) from other sources (see Section 3.4). PMF is a multivariate least-squares technique that constrains the solution to be non-negative and considers the uncertainty of the observed data (Paatero and Tapper, 1994). The PMF methodology included several steps: determining the model parameters, verifying the convergence of the solution to a global minimum, assessing the goodness of the model fit, and estimating the model uncertainties (see details in Krecl et al., 2008 and Krecl et al., 2015). The source identification was conducted through the comparison of modelled PNSD (f-factors) with literature measurements, analysis of the diurnal cycles of the modelled concentrations, and correlation between the factor contributions and observed concentrations at the canyon and rooftop sites (Krecl et al., 2015). Finally, we performed a multiple linear regression (MLR) of the PMF source contributions (g-factors) onto the measured concentrations at the canyon site to calculate the contribution of each source to the observed pollutants (Krecl et al., 2008).

Then, NOx was used as a tracer compound and the average EF for a given species i and fuel type j was computed for the period k ($EF_{i,j,k}$) according to:

$$EF_{i,j,k} = \frac{C_{i,j,k}}{NOx_{j,k}} EF_{NOx,j,k} \tag{2},$$

where $C_{i,j,k}$ is the mean concentration of pollutant i due to emissions of road vehicles burning fuel j in the period k, $NOx_{j,k}$ is the mean NOx concentration attributed to emissions from vehicles driving with fuel j in the period k, and $EF_{NOx,j,k}$ is the weighted EF_{NOx} for all vehicle categories powered by fuel j in the period k.

The target pollutants i were BC, N_4, N_{28}, and size-segregated PN in the interval 28–410 nm, the fuels j were gasoline and diesel, and the periods k were spring 2006 and spring 2013. We obtained $C_{i,j,k}$ and $NOx_{j,k}$ from the PMF and MLR simulations for springs 2006 and 2013, and the EF_{NOx} were extracted from the Handbook Emission Factors for Road Transport (HBEFA) and processed according to the description provided in the next section.

2.2.2. Selection of NOx emission factors

The HBEFA database application estimates the EF of several pollutants per vehicle category, EURO stage, specific year and for a wide variety of traffic situations (Hausberger et al., 2009). The traffic situations are mainly represented by four parameters: area type (rural, urban), road type, road speed limit and service level (free flow, heavy, saturated, and stop and go). HBEFA EF are available for six European countries, including Sweden, and consider their particular national fleet composition and climatic conditions.

In this study, we extracted the EF_{NOx} from the HBEFA V.3.3 handbook (Keller et al., 2017) assuming the national data on EURO stages for each vehicle category and year (that is, 2006 and 2013) and typical site-specific traffic conditions. The traffic situation for the canyon site was chosen for both years as follows: urban, access/residential road type, road speed limit of 50 km h^{-1}, and a specific level of service representative of the inner city streets in Stockholm (free flow 16%, heavy 52%, saturated 28%, and stop and go 4%, VTI, 2006). Then, the EF_{NOx} per vehicle category for each year were weighted according to the vehicle registration for the Stockholm city for the same year. Finally, the EF_{NOx} were grouped into gasoline and fuel vehicles for each year to obtain the variable we defined as $EF_{NOx,j,k}$.

The most recent version of the HBEFA database (V.3.3) updated the EF_{NOx} of diesel passenger cars of the emission standards EURO4, EURO5 and EURO6 considering new laboratory and real-world measurements (portable emission monitoring systems PEMS, and remote sensing data), after compelling evidence that these EF were lower than in-use vehicles studies (Carslaw et al., 2011; Carslaw and Rhys-Tyler, 2013).

The assumption that the HBEFA EF_{NOx} employed in this study corresponds to the real vehicle fleet at the canyon site introduces an uncertainty than can substantially influence the derived particle EF. The Stockholm city vehicle share and emission standard stages at national level can differ from the typical share of the actual fleet driving on the canyon street for the same year. A survey conducted at Hornsgatan site in 2009 analysed automatic number plate recordings of four million vehicles, and provided detailed composition of the fleet share in terms of vehicle categories and EURO stages (Burman and Johansson, 2010). Using the HBEFA V.3.3 database for the year 2009 and the surveyed characteristics, we calculated the EF_{NOx} for the gasoline and diesel real fleets for 2009. We concluded that the real fleet emitted less NOx than the fleet with EURO stages taken from the national statistics and vehicle categories from the Stockholm county registration; this agrees with the Hornsgatan fleet being newer than the national average and with a smaller share of diesel trucks than the city fleet.

Hence, we assumed that in 2006 and 2013 the Hornsgatan fleet was also cleaner in terms of NOx, and reduced the HBEFA EF_{NOx} calculated for 2006 and 2013 by same amount found in 2009 (gasoline: 7.8%, diesel: 37.9%). The offset $EF_{NOx,j,k}$ values were employed in Eq. (2) to finally calculate the particle EF.

3. Results and discussion

3.1. General overview

Because of the role that meteorology plays in the dispersion of atmospheric pollutants and their physico-chemical transformations, we analysed the weather conditions in spring 2006 and 2013 to identify possible differences (Table 1). Both sampling periods presented similar daily mean temperature amplitude and mean daily solar energy dose, with prevailing winds blowing from the southwest and west sectors. However, spring 2013 was slightly more humid and windier than in 2006, and easterly winds were more frequent (21%) than in 2006 (6%).

Pollution measurements were classified as weekday (Mon-Fri) and weekend (Sat-Sun and holidays), and mean concentrations for 2006 and 2013 are displayed in Table 2. Regardless of the sampling period, the mean particle and NOx concentrations were on average 1.5 higher on weekdays than at weekends (Table 2). Comparing

Table 1
Summary of weather conditions during springs 2006 and 2013.

Variable	Spring 2006	Spring 2013
[a]T [°C]	[7.6–15.4]	[8.2–15.3]
[a]RH [%]	[43–82]	[52–92]
[b]WS [m s^{-1}]	3.6	3.8
[c]WD [%]	S (23), W (23), SW (22)	W (22), E (21), SW (11)
[d]Precip. [mm]	45.2	56.2
[e]Precip. [days]	11	14
[f]Solar energy dose [MJ^2]	19.0	19.3

[a] Mean minimum and maximum daily values.
[b] Mean value.
[c] Relative frequency of predominant WD sector.
[d] Cumulative precipitation in the period.
[e] Number of days with precipitation higher than 1 mm.
[f] Mean daily solar energy dose.

pollution levels in 2006 and 2013, we observed a large decrease in concentrations for particulate pollutants on weekdays and weekdays. This reduction was largest for BC mass concentrations (59% on weekdays and 66% at weekends). Kondo et al. (2012) reported an 80% annual decrease in BC concentrations in Tokyo in the period 2003–2010 that were attributed to more stringent regulations of PM emissions from vehicles.

On average, N_4 and N_{28} decreased by 50% and 40%, respectively, with larger reductions on weekdays. The NOx concentrations were slightly higher on weekdays in 2013 than in 2006, whereas a 13% drop was observed at weekends. A study conducted by Carslaw et al. (2011) showed that NO$_x$ concentrations measured at road-side sites tended to remain constant across several European cities over the past few years, coinciding with a larger fraction of diesel vehicles within the passenger car fleet.

In relation to the vehicle fleet, there was a 15.6% traffic reduction at the canyon site and a large shift in vehicle share in the period 2006–2013 (Fig. 1).

The traffic reduction was connected to the introduction of i) a congestion charge in the inner city of Stockholm, first as a trial (from January to July 2006) and permanently since August 2007 (Börjesson et al., 2012), ii) a ban of studded tyres on Hornsgatan street since January 2010. This ban caused a drop in the number of vehicles mainly during the winter tyre season, but the effect partly remained during the rest of the year (Norman et al., 2016). The change in vehicle composition was part of the EU strategy to reduce greenhouse gases emissions and to comply with the Kyoto Protocol (Cames and Helmers, 2013). The share of diesel vehicles increased during the last decade in Sweden, and rose from 18.3% to 48.4% in Stockholm in the period 2006–2013. In 2013, the fraction of diesel cars reached 36.4%, making up two thirds of all new cars in this category. The main driving force for this trend has been national taxation on vehicles and fuels, and CO$_2$ emissions. In Sweden, new vehicles classified as "green cars" were exempted from taxation the first 5 years. This definition only targeted CO$_2$ emissions, and NOx and particle exhaust emissions were not considered.

The introduction of new vehicle technologies in Sweden varied depending on the vehicle category and year (Fig. 2). In 2006, gasoline passenger cars were the largest category (Fig. 1) and

dominated by the most stringent emission standards at that time (Euro 4, Fig. 2a), whereas diesel vehicles presented the highest penetration of the latest emission standards in 2013 (Fig. 2b). In the case of buses and trucks, which were merged into the HD group, the EURO V standards came into force in 2009 and 2010, respectively. For diesel cars, Euro 5 standards were introduced only in 2011 and the continuous expansion of that category explains the high share of this new technology in 2013. After this fleet renewal, the number of vehicles with conventional technology (Euro 0) was very limited in 2013.
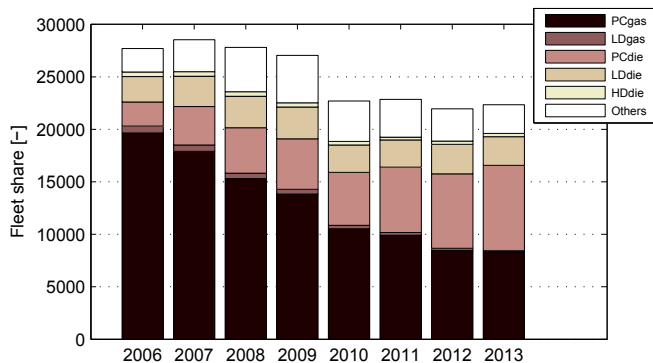
3.2. Diurnal cycles

Fig. 3 shows the mean diurnal variation of particles and NOx concentrations, TR and VS while Fig. 4 displays the mean PNSD profiles for selected hours on weekdays and weekends in springs 2006 and 2013. A hallmark when comparing the diurnal cycles is the large decrease in particle concentrations observed in 2013, especially during daytime on weekdays, and the distinct patterns on weekdays and weekends. The concentrations for both years were significantly higher on weekdays compared to weekends (a Mann-Whitney *U* test was performed at 95% confidence level) between 06:00 and 18:00 h. On weekdays, the concentrations for all pollutants were low during the early hours —when TR was low— and rose abruptly following the increase in TR. Maximum pollution levels were recorded between 07:00 and 09:00 h, matching the high TR and low VS, especially for vehicles driving into the city centre, on the eastbound lane which slopes downwards up to the traffic lights. Thereafter, the concentrations started to decline but did not match the increase of TR in the late afternoon due to a more efficient dispersion within the canyon associated with higher thermal turbulence at that time of the day.

The key features of the diurnal cycles are:

i. In 2013, NOx levels showed no substantial decrease except between 00:00 and 06:00 h (Fig. 3a–b). The morning peak on weekdays was higher than in 2006.
ii. The reduction of BC concentrations in 2013 was significant for all hours. The BC peak observed in the early hours at weekends in 2006 and attributed to exhaust emissions from diesel-fuelled taxis (Krecl et al., 2015) almost disappeared in 2013, suggesting cleaner diesel cars in 2013 than in 2006 (Fig. 3c–d).
iii. There was a substantial decrease for all hours in total an integrated PN concentration for weekdays and weekends (Fig. 3e–h).
iv. A modest decrease in TR was observed between 2006 and 2013 (9.4% on weekdays, and 8.9% at weekends, Fig. 3i–j).
v. The VS for the eastbound lane was significantly lower on weekdays in 2013 (Fig. 3k). This change in driving conditions for the eastbound lane cannot explain the large decrease in PN concentrations in 2013 since deceleration has an opposite effect, increasing PN concentrations in the zone of influence at signalised traffic intersections (Goel and Kumar, 2015). The same study showed that deceleration dropped BC emissions,

Table 2
Hourly mean concentrations for weekdays and weekends in springs 2006 and 2013.

Period	Spring 2006				Spring 2013			
	NOx [μg m^{-3}]	BC [μg m^{-3}]	N$_4$ [cm^{-3}]	N$_{28}$ [cm^{-3}]	NOx [μg m^{-3}]	BC [μg m^{-3}]	N$_4$ [cm^{-3}]	N$_{28}$ [cm^{-3}]
Weekday	128.0	5.1	5.4×10^4	1.2×10^4	128.9	2.1	2.5×10^4	7.0×10^3
Weekend	86.9	3.5	3.8×10^4	8.7×10^3	75.7	1.2	2.1×10^4	5.6×10^3

Fig. 1. Daily mean vehicle share by category at the canyon site for the years 2006–2013. PCgas: gasoline passenger car, LDgas: gasoline light-duty vehicles, PCdie: diesel passenger car, LDdie: diesel light-duty vehicles, HDdie: diesel heavy-duty vehicles, others: ethanol and gas passenger cars, ethanol and gas buses.

3.3. Linear correlations

The Pearson correlation coefficient (R) between the different pollutant concentrations, TR and VS was calculated for hourly averaged data for weekdays and weekends using the Openair package (Fig. 5, Carslaw, 2015). A common feature is the positive correlation between TR and all air pollutants, while VS were negatively correlated, especially on weekdays. Regardless the day of the week, TR and VS were highly anti-correlated, suggesting that the increase in the number of vehicles driving on that street transect reduced the VS. In general, NOx concentrations were highly correlated with particulate pollutants indicating that emissions from traffic exhausts were the common source. TR and pollutant concentrations had lower correlations than between pollutants, since vehicular emissions impact the environmental concentrations of air pollutants non-linearly, as mentioned previously (e.g., the EF depend on vehicle age, terrain characteristics, among others).

Then, we explored the correlation between hourly time series of single channels of PNSD and pollutant concentrations for weekdays and weekends in both years (Fig. 6). In general, the correlations were higher on weekdays than at weekends. NOx was moderately correlated (R > 0.75) with PN concentration in the size range 56–112 nm on weekdays in 2006, when sources are dominated by exhaust emissions. Nickel et al. (2013) found lower correlations (R~0.60) between NOx and PN concentrations in the size range 50–200 nm when analysing vehicle exhausts contributions on a highway in Germany at the end of 2006, whereas Wang et al. (2010) reported higher correlations (R > 0.80) in the size range 10–200 nm at a kerbside site in Copenhagen in spring 2008.

In spring 2006, BC concentrations were moderately correlated (R > 0.75) with PN concentration in the range 56–119 nm irrespective of the day of the week; the maximum correlation (R = 0.87) was found at D_p~113 nm matching the strong unimodal diameter of elemental carbon mass distribution emitted by automobiles (Ning et al., 2013). There is a similar pattern for the correlations between N_4 and PNSD and between N_{28} and PNSD, with the highest correlation at D_p~47 nm.

A larger drop in correlation between the two years was observed for BC and PN concentrations especially for D_p < 200 nm (Fig. 6c–h). Between 2006 and 2013, there was a large increase in the share of diesel passenger cars which came with a number of in-engine measures (e.g., improved fuel injection, exhaust gas recirculation EGR) and after-treatment systems to reduce NOx (e.g., selective catalytic reduction SCR) and particle (e.g., oxidation

but a substantial reduction of BC concentrations was also observed at weekends between 2006 and 2013 with almost no change in the eastbound VS between these two years during daytime.

vi. At weekends, maximum PN concentrations were found later than on weekdays following the TR pattern in the early afternoon (Fig. 4b and d).

vii. On weekdays, the highest PN concentration was observed at 28 nm in 2006 (Fig. 4a) and at 23 nm in 2013 (Fig. 4c) between 08:00 and 09:00 h. At nighttime, the peak diameters were larger compared to the morning hours (33–40 nm in 2006 and 47–58 nm in 2013), with similar PNSD shapes only varying in the number concentration throughout the night. This pattern suggests that the source of particles remained unchanged.

viii. Between 2006 and 2013, there was an overall reduction of N_{28-100} for all hours of the day and irrespective of the day of the week (Fig. 4). The greatest decreases were observed at 08:00 h on weekdays (41%) from 16,280 to 9610 cm^{-3} and at 13:00 h on weekdays and weekends (19%) from 5030 to 4080 cm^{-3}.

ix. On average, N_{28-100} represented 84% of N_{28} on weekdays and weekends for both years, which is in line with several studies that reported UFP contributions up to 90% of the total PN concentration (e.g., Kumar et al., 2010, 2014).
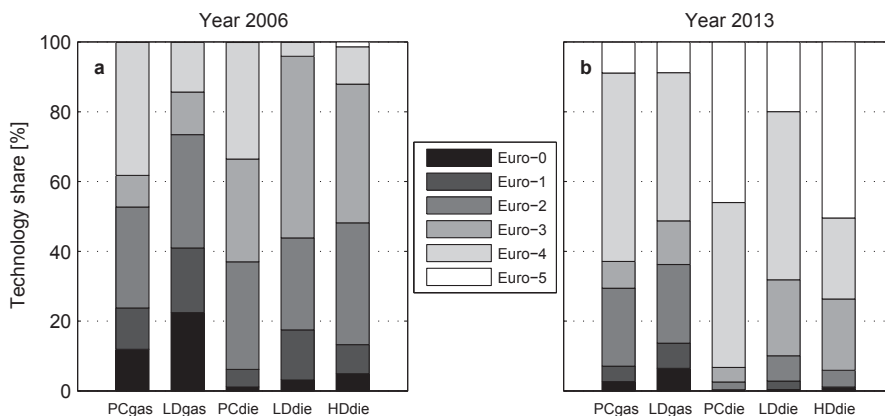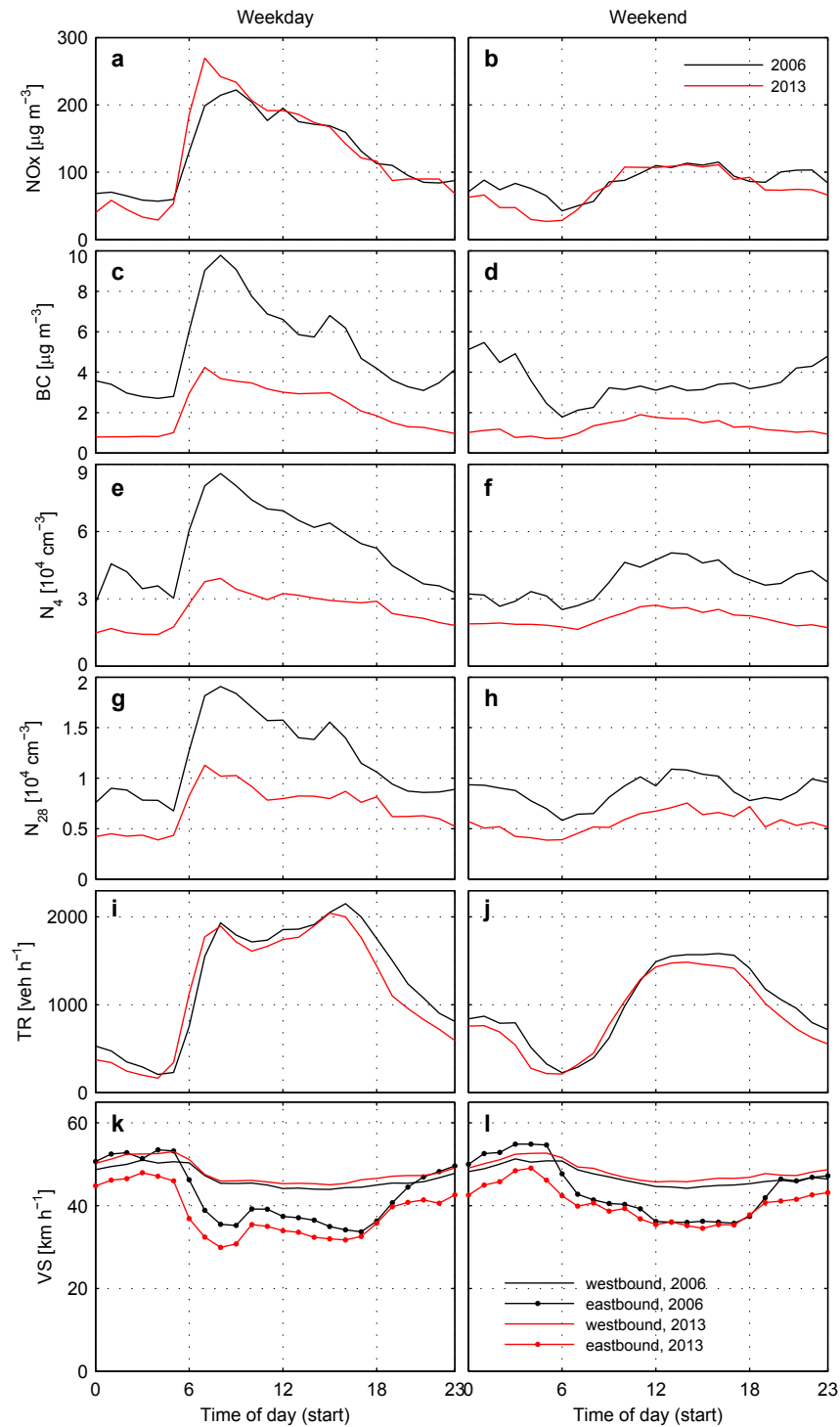

Fig. 2. Fraction of vehicles per category and emission standard stage in Sweden for 2006 (a) and 2013 (b).

Fig. 3. Mean diurnal variation of NOx and several aerosol concentrations, TR and VS for weekdays and weekends in springs 2006 and 2013. Eastbound side indicates driving towards the city centre.

catalysts, and diesel particulate filters DPF) emissions. These new technologies decreased particle emissions in terms of mass and number, but the reduction was not the same for all particle sizes. Fiebig et al. (2014) showed that increasing the injection pressure, controlling the injection timing and using EGR highly reduced the PN concentrations for all sizes, but not in a homogeneous fashion

and Wang et al. (2012) reported that the DPF efficiency depends on the particle size. These advances could explain why the correlations between BC, N_4 and N_{28} with PN concentrations at $D_p < 200$ nm were lower in 2013 when the number of EURO5 diesel cars increased (Figs. 1 and 2).
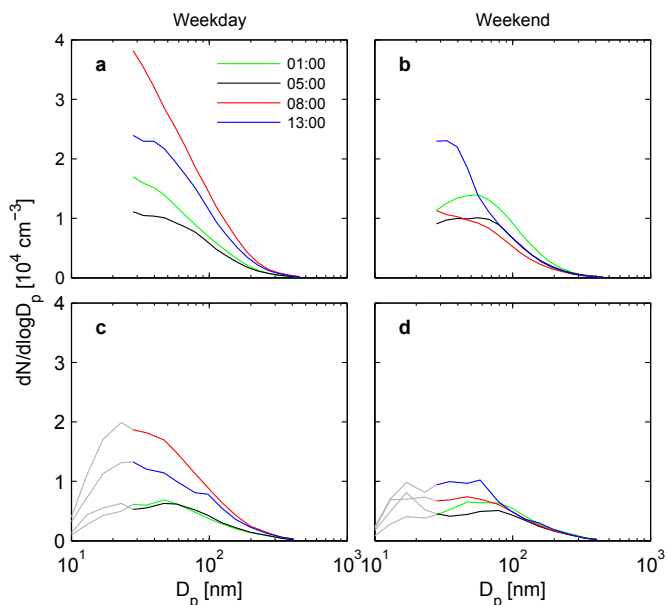
Fig. 4. Mean PNSD on weekdays and weekends for selected times of the day at Hornsgatan site in springs 2006 (a,b) and 2013 (c,d).
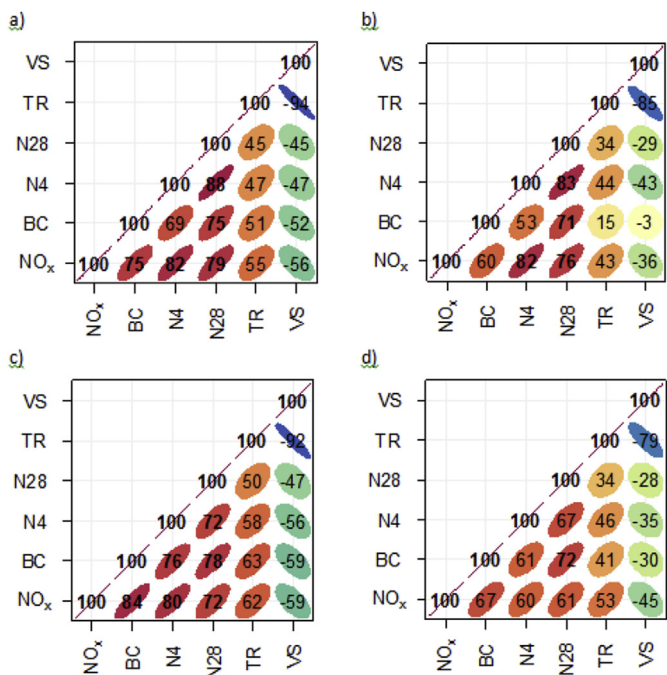

Fig. 5. Pearson correlation matrices of NOx, aerosol variables, TR and VS for weekdays in 2006 (a), weekends in 2006 (b), weekdays in 2013 (c), and weekends in 2013 (d). R = 0.70 are highlighted in bold. The more elliptical and red the form, the larger the positive correlation, while the more elliptical and blue, the larger the negative correlation. (For interpretation of the references to colour in this figure legend, the reader is referred to the web version of this article.)

3.4. PMF results

Fig. 7a–b shows the f-factor profiles for springs 2006 and 2013 while Fig. 7c–h displays the correlations between the modelled N_{28} concentrations and observed $dN/dlogD_p$. We also analysed the linear correlation between simulated N_{28} concentrations and co-pollutants measured at the canyon and rooftop sites.
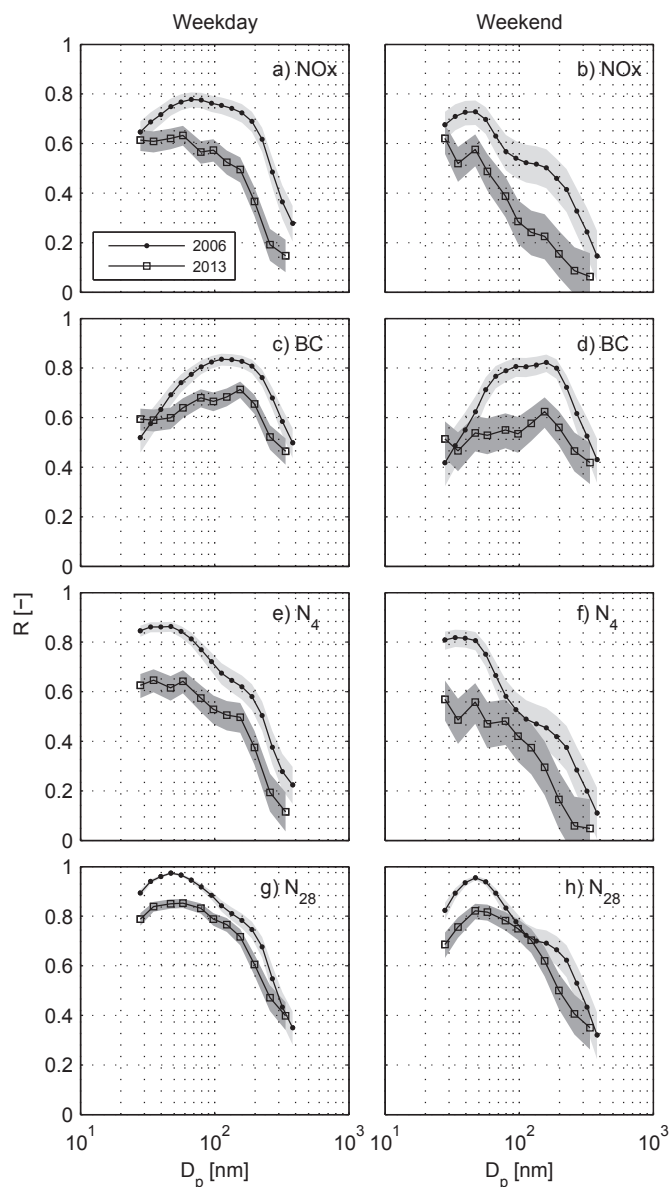

Fig. 6. Pearson correlation between NOx and particle concentrations per size bin for weekdays and weekends in springs 2006 and 2013. Shaded areas represent 95% confidence interval for R: light gray (2006) and dark gray (2013). Note that for 2013, subplots e-f and g-h represent the correlation between N_4 and PNSD, and between N_{28} and PNSD per size bin, respectively.

F-factor 1 was dominated by UFP with maximum concentrations of 1.6×10^4 and 6.4×10^3 cm^{-3} at D_p ~28 nm in 2006 and 2013, respectively. The shapes of these f-factors were similar to the PNSD observed during the morning weekdays when the canyon was very busy, and the simulated N_{28} for factor 1 was highly correlated with small particles on weekdays and at weekends (Fig. 7c,f). Note that even though the peak reported at 28 nm was limited by the lower limit of the DMPS coincident interval in 2006 and 2013, the real peak was smaller than 30 nm and, according to Imhof et al. (2005), corresponds to primary and secondary particles from exhausts of a mixed fleet (gasoline and diesel engines). Due to the low correlation between the modelled N_{28} for f-factor 1 and BC and the moderate correlations with NOx and CO (not shown), we suggest that factor 1 was dominated by emissions from gasoline engines.

F-factor 2 peaked at 67 nm in 2006 (5.6×10^3 cm^{-3}) and at
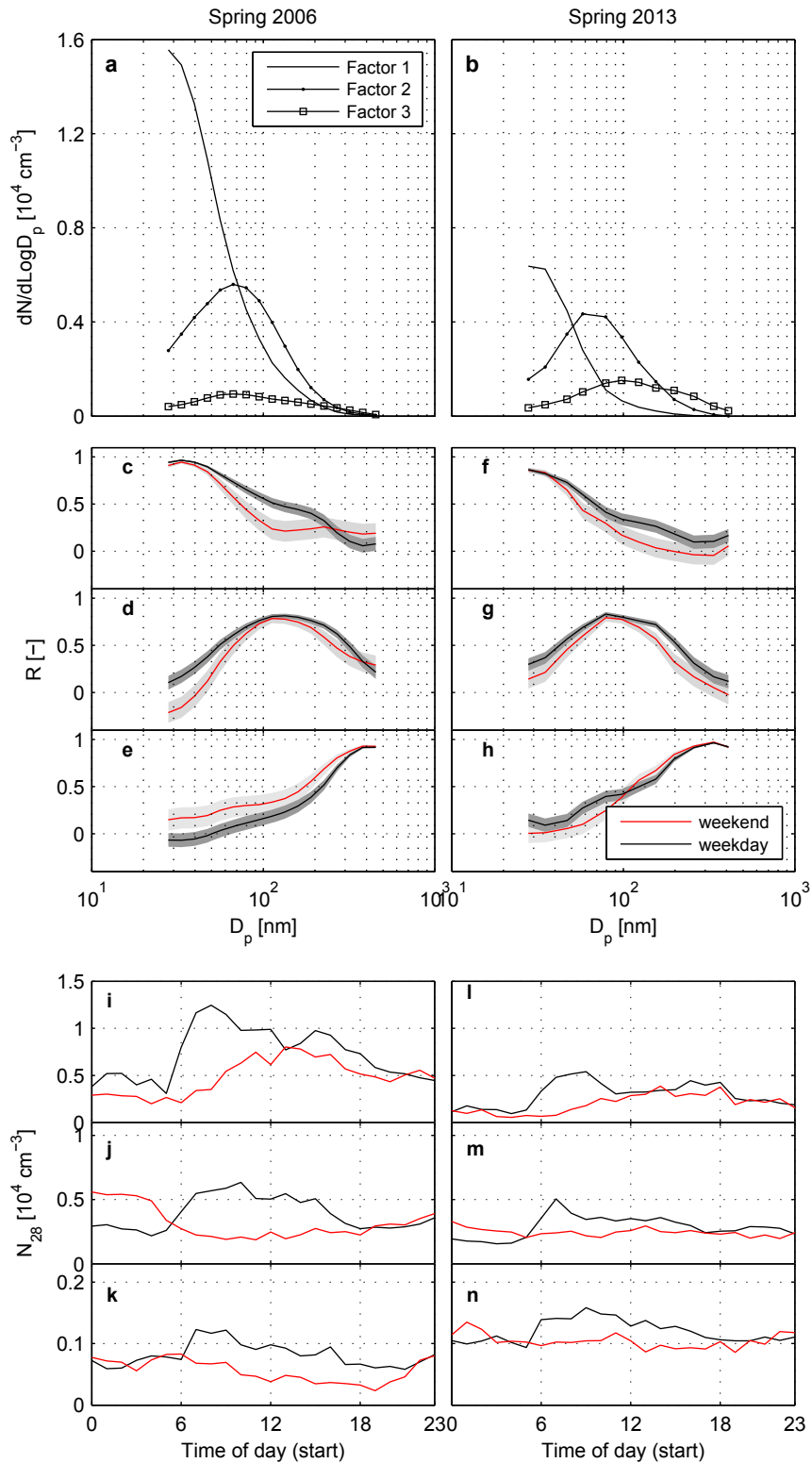
Fig. 7. F-factor profiles (a–b), modelled diurnal variation of N_{28} on weekdays and weekends for factor 1 (c,f), factor 2 (d,g) and factor 3 (e,h), and the linear correlation between modelled N_{28} and observed $dN/dlogD_p$ on weekdays and weekends for factor 1 (i,l), factor 2 (j,m) and factor 3 (k,n). Shaded areas represent 95% confidence intervals for R: light gray (weekends) and dark gray (weekdays).

58 nm in 2013 (4.3×10^3 cm^{-3}), and displayed larger N_{28} concentrations at weekends than on weekdays in the early hours of both years. Furthermore, it was associated with particles in the D_p range 95–160 nm (Fig. 7d,g), NOx and BC, but not correlated with CO (not

shown). Ntziachristos et al. (2007) and Gouriou et al. (2004) found a PNSD mode at 70–100 nm when sampling ambient air close to motorways with large fraction of diesel traffic. Thus, we attributed f-factor 2 to exhaust emissions from diesel vehicles. The mode shift

for f-factor 2 between 2006 and 2013 and the reduction in concentrations could be explained by the introduction of in-engine measures (Section 3.3).

F-factor 3 peaked at 67 nm (concentration of 940 cm^{-3}) in 2006 and at 98 nm (concentration of 1518 cm^{-3}) in 2013. Modelled N_{28} values for factor 3 might be influenced by local human sources since they were significantly higher on weekdays than at weekends for daytime for both years (unpaired t-test, 95% confidence interval). F-factor 3 was weakly or no correlated with measurements conducted at street level, but higher R values were obtained when modelled N_{28} concentrations were correlated with rooftop observations, especially for BC (not shown). Since f-factor 3 was highly correlated with accumulation mode particles (Fig. 7e,h), we attributed this factor to the urban background contribution, including aged aerosol emitted from combustion processes in the city and long-range transported particles (Vu et al., 2015).

For both years, the modelled N_{28} concentrations for f-factors 1 and 2 show a regular rush-hour cycle during weekdays and weekends, suggesting that particles were mainly emitted by vehicle exhausts very close to the measurement site. N_{28} concentrations for f-factor 3 showed no clear diurnal cycle, which reinforces that its sources were not local (Fig. 7i–n).

We performed a linear regression analysis between modelled and observed BC, N_4, N_{28}, and NOx concentrations to assess the goodness of the model fit. We found high correlations (R > 0.75) for all variables in both years. Table 3 displays the modelled NOx, BC, N_4 and N_{28} concentrations attributed to gasoline and diesel vehicle emissions in 2006 and 2013. There was an overall reduction of concentrations for gasoline and diesel vehicles when comparing 2006 and 2013. A large decrease was found for particulate pollutants attributed either to gasoline or diesel emissions, and remarkably for BC concentrations. In 2006, PN concentrations were dominated by gasoline-powered vehicles whereas in 2013 the contribution of diesel vehicles is very similar to the gasoline fleet.

3.5. Calculated EF and comparison with other studies

Emission factors for PN for various size intervals and BC were derived for the gasoline and diesel fleets using the PMF method combined with EF_{NOx} from the HBEFA database (Table 4). In general, EF for 2013 were always lower than the ones derived for 2006 which is in line with the various technological improvements implemented to decrease particle exhaust emissions. The reduction in EF_{BC} was 77% for gasoline and diesel vehicles, whereas the reduction was highest for EF_{PN} for the gasoline fleet (77–82%) when compared to the diesel fleet (37–44%). For both years and all pollutants, the EF for the diesel fraction were always higher than those for the gasoline fleet, which is consistent with the literature (Kumar et al., 2011 and references therein).

Our real-world EF were higher than the weighted EF_{PN} by vehicle category and fuel type calculated using the HBEFA database (Table 4). The large difference between EF_{N4} and EF_{N28} indicates an important contribution of very small particles to the total PN emitted by vehicles. The large difference between EF_{N28} and EF_{N23} could be explained by the on-road method measuring primary and secondary particles and the laboratory measurements only accounting for primary emissions. Note that the EF_{PN} from HBEFA represent non-volatile particles according to the protocol of the Particulate Measurement Programme (PMP), i.e. 50% particle cut-off at 23 nm and hot dilution of the sample probe. Normally the volatile parts of the particles are removed using a heated dilution stage (150 °C) and a heated tube (at 300–400 °C) (Giechaskiel et al., 2010). This means that only part of the emitted particles will finally reach the CPC in laboratory tests. Note also that the lower cut-off is different (23 nm and 28 nm), and that the HBEFA EF_{PN} have large uncertainty, high variability of tests results within a single laboratory and are very sensitive to the status of the DPF and to engine operation conditions (Hausberger et al., 2014).

In the case of BC, the measured EF_{BC} for the gasoline fleet was a factor of 8–22 higher than the TRANSPHORM database (Table 4). Conversely, the average EF_{BC} for the diesel vehicles in 2006 and 2013 were very similar to the database values for both years. The same behaviour for the gasoline and diesel EF_{BC} was observed by Liggio et al. (2012) when conducting on-road measurements on a major highway in Canada in 2010, reporting that the on-road EF_{BC} was nine-fold higher than the database value for gasoline vehicles. EF_{BC} from the TRANSPHORM database were derived from $EF_{PM2.5}$ calculated by COPERT using the BC/$PM_{2.5}$ ratios suggested by Ntziachristos and Kouridis (2007) for different vehicle categories, and uncertainties were estimated in the 10–50% range (Vouitsis et al., 2013). The results of HBEFA and COPERT emission models are verified by a vast set of laboratory tests, and the differences between laboratory-based and real-world EF could be attributed to non-representative dynamometer test conditions compared to real-world driving conditions (Jamriska and Morawska, 2001) and, in the case of PN, different size range coverage, and non-volatile versus volatile PNC measurements.

Direct comparison with other studies conducted under real-world conditions is difficult because they usually report EF for a mixed fleet or split between LDV and HDV, whereas we segregated by fuel type. Besides, the vehicle technology stage is different from this work. The share between LDV and HDV did not change in Sweden between 2006 and 2013, but the gasoline and diesel fleet fractions were drastically modified as previously commented. In 2006, the gasoline and LDV shares represented 79.8% and 94.5% of the total fleet, respectively. In 2013, the gasoline fleet in Stockholm decreased to 48.4% and the diesel share went up to 42.9% of the total fleet. Thus, our gasoline EF should be lower than LDV EF for the same conditions since diesel LDV EF are higher than gasoline LDV (Kumar et al., 2011) and our diesel EF should be lower than the HDV EF because diesel includes LDV that have lower EF than HDV (Kumar et al., 2011). However, EF depend also on other factors than the fuel type such as vehicles age, driving conditions, meteorology, measurement and computation techniques. Our results are within the range of LDV and HDV EF reviewed by Kumar et al. (2011). Studies on the on-road EF trends are very scarce; a decreasing trend in EF_{PN} was also observed in Copenhagen between 2001 and 2008 for the mixed vehicle fleet (from 2.8 × 10^{14} to 2.15 × 10^{14} km^{-1} veh^{-1}) when measuring PNC in the range 10–700 nm and a 5–7% HDV fraction (Ketzel et al., 2003; Wang et al., 2010).

Our EF_{BC} for gasoline were within the range of LDV EF measured in tunnels (3.2–17.8 mg km^{-1} veh^{-1}) and the diesel EF were lower than the HDV EF value (131.0 mg km^{-1} veh^{-1}) as reviewed by Zhang et al. (2015). To compare our results with on-road EF segregated by fuel type, we weighted the EF_{BC} measured by Ježek et al. (2015) for different categories and fuels on Slovenian motorways by the fraction of vehicles on that category and fuel at the canyon site for 2006 and 2013. The computed EF for gasoline were [10.5–32.2] mg km^{-1} veh^{-1} for both years, and for diesel [57.6–156.0] and [26.8–86.3] mg km^{-1} veh^{-1} in 2006 and 2013, respectively. Our on-

Table 3
Concentrations of NOx, BC, N_4, and N_{28} attributed to diesel and gasoline powered vehicles after PMF results for 2006 and 2013.

Fuel type	NOx [µg m^{-3}]	BC [µg m^{-3}]	N_4 [10^4 cm^{-3}]	N_{28} [10^3 cm^{-3}]
Gasoline 2006	59.3	1.6	2.9	6.4
Gasoline 2013	57.6	0.7	0.9	2.6
Diesel 2006	46.5	2.3	1.4	3.7
Diesel 2013	42.7	0.7	0.9	2.7

Table 4
EF of total and integrated PN and BC per vehicle for gasoline and diesel fleets for 2006 and 2013 calculated using PMF results and using EF from the HBEFA and TRANSPHORM databases. EF_{NOx} used for the calculations are also displayed.

Species	Reference	Gasoline 2006	Gasoline 2013	Diesel 2006	Diesel 2013
N_4 [10^{12} km^{-1} veh^{-1}]	This study	193.2	35.2	591.2	333.4
N_{28} [10^{12} km^{-1} veh^{-1}]	This study	42.9	10.0	153.3	96.4
[a]N_{23} [10^{12} km^{-1} veh^{-1}]	HBEFA V.3.3	1.6	0.8	94.2	30.4
BC [mg km^{-1} veh^{-1}]	This study	11.0	2.5	94.8	23.4
BC [mg km^{-1} veh^{-1}]	TRANSPHORM	0.5	0.3	92.9	23.8
NOx [mg km^{-1} veh^{-1}]	HBEFA V.3.3	396.6	218.3	1948.4	1510.0

[a] HBEFA considers non-volatile particles with Dp $\geq$ 23 nm.

road EF_{BC} were within these ranges, but for the gasoline fraction in 2013, which is much lower. Note that the Slovenian EF_{BC} were derived from an older fleet since measurements were conducted in 2011.

Fig. 8 shows size-resolved EF_{PN} for gasoline and diesel vehicles in 2006 and 2013. Regardless of the fuel type and particle size, PN distinctly decreased from 2006 to 2013. This finding is consistent with the observed reduction of submicrometer particles between these two years (Fig. 4). Irrespective of the year, the importance of the gasoline fleet as a PN emission source increases for smaller D_p (maximum at 28 nm), whereas the highest diesel fleet contribution is observed at 67 nm. Note that the present study covers the size range 28–410 nm and the EF for the gasoline and diesel fleets could have peaked below the lower cut-off size. Diesel vehicles emit more particles than gasoline engines for all particles sizes measured, reaching one order of magnitude difference. The shape of the gasoline EF size distribution shows a reasonable agreement with the measured for LDV vehicles in a Stockholm tunnel in 1999 at a VS of 50 km h^{-1} (Kristensson et al., 2004), since the LDV fraction was dominated by gasoline vehicles in 1999. As expected, the absolute numbers were highest in 1999 and lowest in 2013 for all size bins. A direct comparison between diesel and diesel HDV EF is more challenging because the diesel fraction also contains LDV, and this fraction largely varied between 2006 and 2013. Size-resolved EF_{PN} for diesel HDV in 1999 (Kristensson et al., 2004) peaked at 30 nm and a second mode was found at ~80 nm when the VS was 50 km h^{-1} whereas we observed one mode at 67 nm for both years.
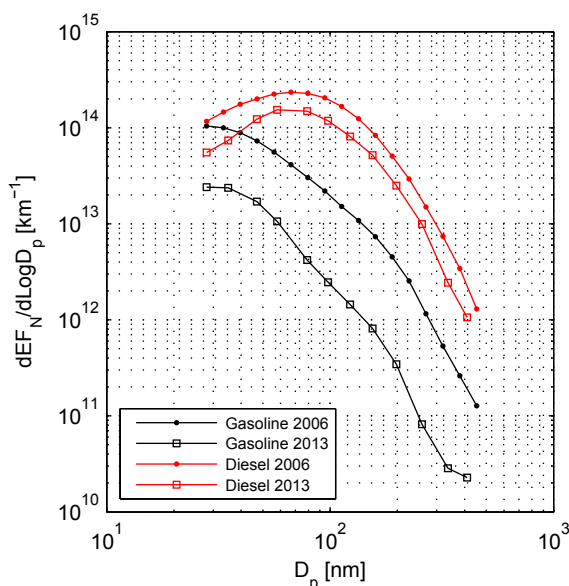

Fig. 8. Size-resolved EF_{PN} for the gasoline and diesel fleets in 2006 and 2013.

Observe that we derived the vehicle EF from measurements conducted during springtime in Stockholm and caution should be taken in the overall use of these EF. Due to the seasonality effects on particle formation (increase in the UFP number fraction for low temperatures, e.g., Olivares et al., 2007) and catalyst malfunction when below its light-off temperature most likely due to cold-start conditions in wintertime (Eastwood, 2008), the validity of the derived EF should be interpreted in the application context. In the case of particle number EF, the values were reported for $D_p \geq 4$ and 28 nm and size-resolved in the interval 28–410 nm, thus, not being suitable for EF determination of UFP.

3.6. Traffic particulate emissions per fuel type

For the years 2006 and 2013, the emissions of BC, N_4 and N_{28} were computed per day and km driven on Hornsgatan street for the gasoline and diesel fleets. The calculations considered the daily mean TR weighted by the corresponding fuel fraction and the EF derived from this study and from the TRANSPHORM (BC) and HBEFA (N_{23}) databases; the results are displayed in Fig. 9.

Regardless of the different EF used for these calculations, the total traffic emissions in 2013 were lower than in 2006 reflecting the improvements in vehicle technology to reduce particle emissions. For both years, BC emissions were higher for the diesel than for the gasoline fleet. Conversely, the gasoline fleet emitted more particles (N_4 and N_{28}) than the diesel fleet in 2006, when the gasoline fraction dominated the share (see Section 3.1). In 2013, after the rapid dieselisation process, the PN emissions from the diesel fleet exceeded that from gasoline vehicles. These findings suggest that the different measures adopted to decrease particle emissions (e.g., DPF systems) were more successful in reducing particle mass (measured here through BC mass) than PN in diesel vehicles.

In 2006, the traffic emissions of BC, N_4 and N_{28} per day and km driven calculated with the EF derived from this study were 723 g, 7.3 $\times$ 10^{18} and 1.7 $\times$ 10^{18} particles, respectively; the diesel fleet contributed with 66%, 45% and 41% of the total emissions, respectively. The largest reduction in total daily emissions between 2006 and 2013 was observed for BC (61%), when both gasoline and diesel fleets decreased their contributions (Fig. 9a). Different from BC, there was an overall reduction of 34–45% for the number of particles between the two years but the diesel emissions increased 21–35% in 2013 (Fig. 9b–c). Even though the diesel EF_{PN} for all particle sizes were lower than before (Fig. 8), the number of diesel vehicles was higher in 2013 than in 2006 (Fig. 2) and in total emitted more particles with smaller diameters that contributed greatly to the number but not much to the BC mass.

When using EF from the databases, the emissions from the gasoline fleet were much lower for all pollutants in both years (Fig. 9a,c). For the diesel fleet, the BC emissions were very similar (Fig. 9a), but the PN emissions were 38–68% lower than when on-road EF were used (Fig. 9c). Thus, the use of EF based on laboratory
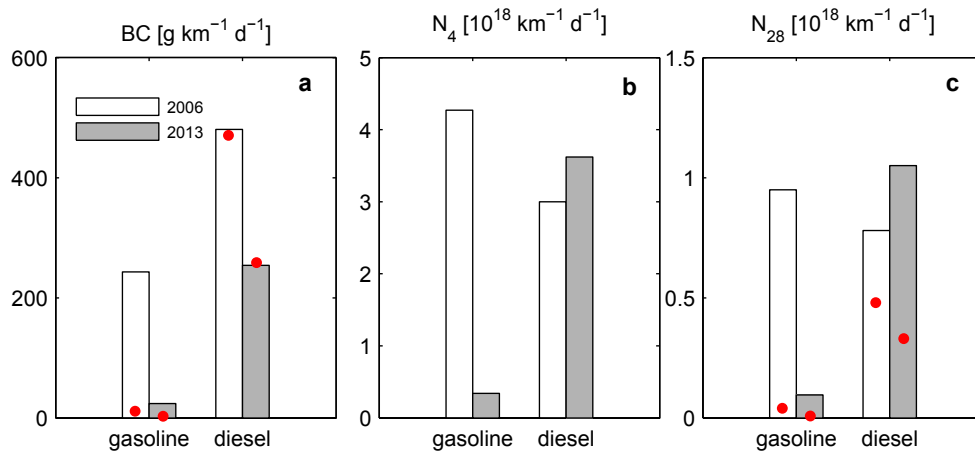
Fig. 9. Daily emissions of BC, N_4 and N_{28} for gasoline and diesel fleets per km driven on Hornsgatan street in 2006 and 2013 using the EF calculated in this study. The red dots represent the values derived from the emission databases: TRANSPHORM for BC (a), and HBEFA V3.3 for N_{23} (c). (For interpretation of the references to colour in this figure legend, the reader is referred to the web version of this article.)

driving cycles should be used with care both for BC mass and PN. Modelling results using database EF need to be interpreted considering the risks that emissions could be underestimated, and preferably site-specific real-world emission measurements should be undertaken.

4. Conclusions

This study analysed kerbside measurements of NOx, BC, and total and size-resolved PNC in Stockholm in 2006 and 2013, and by applying a novel combination of the tracer method with a multi-variate factor analysis, EF were calculated for the fuel-segregated vehicle fleet. Between these two years, there was a strong diesel-isation process of the light-duty fleet —as observed in many European countries— and several technological improvements to meet the strict emission standards for new vehicles.

These changes in the vehicle fleet caused a clear reduction in the ambient concentration of particulate pollutants irrespective of the day of the week and the time of the day, whereas NOx concentrations remained rather constant as found in other European cities. However, translating this into new viable EF still proved to be a challenge in this field of work.

The EF_{BC} and size-segregated EF_{PN} derived for the Swedish fleet in urban conditions, with frequent stop-and-go situations, were consistent with on-road factors measured in other countries. However, our EF_{PN} (gasoline and diesel) and EF_{BC} (only gasoline) were much higher than the EF simulated with traffic emission models validated with laboratory tests. This finding suggests that the EF from the two leading models (HBEFA and COPERT) in Europe should be revised for BC (gasoline vehicles) and PN (all vehicles), since they are used to compile official national inventories for the road transportation sector and also assess their associated health impacts.

It is clear from the current work that the EURO standards limits and improved technologies for new vehicles have been successful in reducing the BC mass and number of particles emitted by traffic and also their ambient concentrations. Finally, this work also highlighted the importance of long-term observations to detect trends, assess the effectiveness of regulations to improve the urban air quality, and validate emission estimates based on laboratory tests.

References

Bond, T.C., Anderson, T.L., Campbell, D., 1999. Calibration and intercomparison of filter-based measurements of visible light absorption by aerosols. Aerosol Sci. Technol. 30, 582—600.

Bond, T.C., Doherty, S.J., Fahey, D.W., Forster, P.M., Berntsen, T., De Angelo, B.J., Flanner, M.G., Ghan, S., Kärcher, B., Koch, D., Kinne, S., Kondo, Y., Quinn, P.K., Saro, M.C., Schultz, M.G., Venkataraman, C., Zhang, H., Zhang, S., Bellouin, N., Guttikunda, S.K., Hopke, P.K., Jacobson, M.Z., Kaiser, J.W., Klimont, Z., Lohmann, U., Schwarz, J.P., Shindell, D., Storelvmo, T., Warren, S.G., Zender, C.S., 2013. Bounding the role of black carbon in the climate system: a scientific assessment. J. Geophys. Res. 118, 5380—5552.

Börjesson, M., Eliasson, J., Hugosson, M.B., Brundell-Freij, K., 2012. The Stockholm congestion charge -5 years on. Effects, acceptability and lessons learnt. Transp. Policy 20, 1—12.

Burman, L., Johansson, C., 2010. Emissions and Concentrations of Nitrogen Oxides and Nitrogen Dioxide on Hornsgatan Street; Evaluation of Traffic Measurements during Autumn 2009 (In Swedish Only). SLB Report 7. http://slb.nu/slb/rapporter/pdf8/slb2010_007.pdf.

Cames, M., Helmers, E., 2013. Critical evaluation of the European diesel car boom - global comparison, environmental effects and various national strategies. Environ. Sci. Eur. 25, 15.

Carslaw, D.C., 2015. The Openair Manual - Open-source Tools for Analysing Air Pollution Data. Manual for Version 1.1-4. King's College London.

Carslaw, D.C., Rhys-Tyler, G., 2013. New insights from comprehensive on-road measurements of NOx, NO2 and NH3 from vehicle emission remote sensing in London, UK. Atmos. Environ. 81, 339—347.

Carslaw, D.C., Beevers, S.D., Tate, J.E., Westmoreland, E., Williams, M.L., 2011. Recent evidence concerning higher NOx emissions from passenger cars and light duty vehicles. Atmos. Environ. 45, 7053—7063.

Chung, Y., Dominici, F., Wang, Y., Coull, B., Bell, M., 2015. Associations between long-term exposure to chemical constituents of fine particulate matter (PM2.5) and mortality in medicare enrollees in the Eastern United States. Environ. Health Perspect. 123, 467—474.

Drinovec, L., Močnik, G., Zotter, P., Prévôt, A.S.H., Ruckstuhl, C., Coz, E., Rupakheti, M., Sciare, J., Müller, T., Wiedensohler, A., Hansen, A.D.A., 2015. The "dual-spot" aethalometer: an improved measurement of aerosol black carbon with real-time loading compensation. Atmos. Meas. Tech. 8, 1965—1979.

Eastwood, P., 2008. Particulate Emissions from Vehicles. John Wiley & Sons, Ltd., England. ISBN 978-0-7680-2060-1.

EEA, 2015a. Air Quality in Europe - 2015 Report. EEA Technical Report No 5/2015, ISSN 1977—8449. http://www.eea.europa.eu/publications/air-quality-in-europe-2015.

EEA, 2015b. European Union Emission Inventory Report 1990—2013 under the

UNECE Convention on Long-range Transboundary Air Pollution (LRTAP). http://dx.doi.org/10.2800/031449. EEA Technical report No 8/2015, ISBN 978-92-9213-655-0. http://www.eea.europa.eu/publications/lrtap-emission-inventory-report.

EMEP, 2013. EMEP/EEA Air Pollutant Emission Inventory Guidebook 2013. http://dx.doi.org/10.2800/92722. ISSN 1725–2237. http://www.eea.europa.eu/publications/emep-eea-guidebook-2013.

Fiebig, M., Wiartalla, A., Holderbaum, B., Kiesow, S., 2014. Particulate emissions from diesel engines: correlation between engine technology and emission. J. Occup. Med. Toxicol. 9 http://dx.doi.org/10.1186/1745-6673-9-6.

Franco, V., Kousoulidou, M., Muntean, M., Ntziachristos, L., Hausberger, S., Dilara, P., 2013. Road vehicle emission factors development: a review. Atmos. Environ. 70, 84–97.

Fuzzi, S., Baltensperger, U., Carslaw, K., Decesari, S., Denier Van Der Gon, H., Facchini, M.C., Fowler, D., Koren, I., Langford, B., Lohmann, U., Nemitz, E., Pandis, S., Riipinen, I., Rudich, Y., Schaap, M., Slowik, J.G., Spracklen, D.V., Vignati, E., Wild, M., Williams, M., Gilardoni, S., 2015. Particulate matter, air quality and climate: lessons learned and future needs. Atmos. Chem. Phys. 15, 8217–8299. ISSN 1680–7316.

Giechaskiel, B., Chirico, R., DeCarlo, P.F., Clairotte, M., Adam, T., Martini, G., Heringa, M.F., Richter, R., Prevot, A.S.H., Baltensperger, U., Astorga, C., 2010. Evaluation of the particle measurement programme (PMP) protocol to remove the vehicles' exhaust aerosol volatile phase. Sci. Total Environ. 408, 5106–5116.

Goel, A., Kumar, P., 2015. Zone of influence for particle number concentrations at signalized traffic intersections. Atmos. Environ. 123, 25–38.

Gouriou, F., Morin, J.P., Weill, M.E., 2004. On-road measurements of particle number concentrations and size distributions in urban and tunnel environments. Atmos. Environ. 38, 2831–2840.

Hausberger, S., Rexeis, M., Kühlwein, J., Luz, R., 2014. Update of Emission Factors for EURO 5 and EURO 6 Vehicles for the HBEFA Version 3.2. Final Report, Report No. I-31/2013/Rex EM-I 2011/20/679. http://www.hbefa.net/e/documents/HBEFA32_EF_Euro_5_6_TUG.pdf.

Hausberger, S., Rexeis, M., Zallinger, M., Luz, R., 2009. Emission Factors from the Model PHEM for the HBEFA Version 3, Institute for Internal Combustion Engines and Thermodynamics. Graz University of Technology. Report Nr. I-20a/2009 Haus-Em 33a/08/679.

HEI, 2013. HEI Review Panel on Ultrafine Particles. Understanding the Health Effects of Ambient Ultrafine Particles. HEI Perspectives 3. Health Effects Institute, Boston, MA, 2013122. http://pubs.healtheffects.org/getfile.php?u=893.

Imhof, D., Weingartner, E., Ordonez, C., Gehrig, R., Hill, M., Buchmann, B., Baltensperger, U., 2005. Real world emission factors of fine and ultrafine aerosol particles for different traffic situations in Switzerland. Environ. Sci. Technol. 39, 8341–8350.

Jamriska, M., Morawska, L., 2001. A model for determination of motor vehicle emission factors from on-road measurements with a focus on submicrometer particles. Sci. Total Environ. 264, 241–255.

Janssen, N.H.A., Gerlofs-Nijla, M.E., Lanki, T., Salonen, R.O., Cassee, F., Hoek, G., Fischer, P., Brunekreed, B., Krzyzanowsk, M., 2012. Health effects of black carbon. World Health Organization, Regional Office for Europe.

Ježek, I., Katrašnik, T., Westerdahl, D., Mocnik, G., 2015. Black carbon, particle number concentration and nitrogen oxide emission factors of random in-use vehicles measured with the on-road chasing method. Atmos. Chem. Phys. 15, 11011–11026.

Keller, M., Hausberger, S., Matzer, C., Wüthrich, P., Notter, B., 2017. HBEFA 3.3 – Update of NOX Emission Factors of Diesel Passenger Cars- Background Documentation. http://www.hbefa.net/e/documents/HBEFA33_Documentation_20170425.pdf.

Ketzel, M., Berkowicz, R., 2004. Modelling the fate of ultrafine particles from exhaust pipe to rural background: an analysis of time scales for dilution, coagulation and deposition. Atmos. Environ. 38, 2639–2652.

Ketzel, M., Wåhlin, P., Berkowicz, R., Palmgren, F., 2003. Particle and trace gas emission factors under urban driving conditions in Copenhagen based on street and roof-level observations. Atmos. Environ. 37, 2735–2749.

Kondo, Y., Rama, K., Takegawa, N., Sahuc, L., Morino, Y., Liu, X., Oharad, T., 2012. Reduction of black carbon aerosols in Tokyo: comparison of real-time observations with emission estimates. Atmos. Environ. 54, 242–249.

Krecl, P., Hedberg Larsson, E., Ström, J., Johansson, C., 2008. Contribution of residential wood combustion and other sources to hourly winter aerosol in northern Sweden determined by Positive Matrix Factorization. Atmos. Chem. Phys. 8, 3639–3653.

Krecl, P., Targino, A.C., Johansson, C., 2011. Spatiotemporal distribution of light-absorbing carbon and its relationship to other atmospheric pollutants in Stockholm. Atmos. Chem. Phys. 11, 11553–11567.

Krecl, P., Targino, A.C., Johansson, C., Ström, J., 2015. Characterisation and source apportionment of submicron particle number size distributions in a busy street canyon. Aerosol Air Qual. Res. 15, 220–233.

Krecl, P., Targino, A.C., Wiese, L., Ketzel, M., Correa, M.P., 2016. Screening of short-lived climate pollutants in a street canyon in a mid-sized city in Brazil. Atmos. Pollut. Res. 7, 1022–1036.

Kristensson, A., Johansson, C., Westerholm, R., Swietlicki, E., Gidhagen, L., Wideqvist, U., Vesely, V., 2004. Real-world traffic emission factors of gases and particles measured in a road tunnel in Stockholm, Sweden. Atmos. Environ. 38, 657–673.

Kumar, P., Morawska, L., Birmili, W., Paasonen, P., Hu, M., Kulmala, M., Harrison, R.M., Norford, L., Britter, R., 2014. Ultrafine particles in cities. Environ. Int. 66, 1–10.

Kumar, P., Robins, A., Vardoulakis, S., Britter, R., 2010. A review of the characteristics of nanoparticles in the urban atmosphere and the prospects for developing regulatory controls. Atmos. Environ. 44, 5035–5052.

Kumar, P., Ketzel, M., Vardoulakis, S., Pirjola, L., Britter, R., 2011. Dynamics and dispersion modelling of nanoparticles from road traffic in the urban atmospheric environment – a review. J. Aerosol Sci. 42, 580–603.

Liggio, J., Gordon, M., Smallwood, G., Li, S.-M., Stroud, C., 2012. Are emissions of black carbon from gasoline vehicles underestimated? Insights from near and on-road measurements. Environ. Sci. Technol. 46, 4819–4828.

Maher, B.A., Ahmed, I.A.M., Karloukovski, V., MacLaren, D.A., Foulds, P.G., Allsop, D., Mann, D.M.A., Torres-Jardón, R., Calderon-Garciduenas, L., 2016. Magnetite pollution nanoparticles in the human brain. PNAS 113 (39), 10797–10801.

Nickel, C., Kaminski, H., Hellack, B., Quass, U., John, A., Klemm O., Kuhlbusch, T.A.J., 2013. Size resolved particle number emission factors of motorway traffic differentiated between heavy and light duty vehicles. Aerosol Air Qual. Res. 13, 450–461.

Ning, Z., Chan, K.L., Wong, K.C., Westerdahl, D., Mocnik, G., Zhou, J.H., Cheung, C.S., 2013. Black carbon mass size distributions of diesel exhaust and urban aerosols measured using differential mobility analyzer in tandem with aethalometer. Atmos. Environ. 80, 31–40.

Norman, M., Sundvor, I., Denby, B.R., Johansson, C., Gustafsson, M., Blomqvist, G., Janhäll, S., 2016. Modelling road dust emission abatement measures using the NORTRIP model: vehicle speed and studded tyre reduction. Atmos. Environ. 134, 96–108.

Ntziachristos, L, Kouridis, C., 2007. EMEP Corinair Emissions Inventory Guidebook 2007. Group 7 — Road Transport. http://reports.eea.europa.eu/EMEPCORINAIR5/.

Ntziachristos, L., Ning, Z., Geller, M.D., Sioutas, C., 2007. Particle concentration and characteristics near a major freeway with heavy-duty diesel traffic. Environ. Sci. Technol. 41, 2223–2230.

Olivares, G., Johansson, C., Ström, J., Hansson, H.-C., 2007. The role of ambient temperature for particle number concentrations in a street canyon. Atmos. Environ. 41, 2145–2215.

Paatero, P., Tapper, U., 1994. Positive Matrix Factorization: a non-negative factor model with optimal utilization of error estimates of data values. Environmetrics 5, 111–126.

Petzold, A., Kramer, H., Schönlinner, M., 2002. Continuous measurement of atmospheric black carbon using a multi-Angle absorption photometer. Environ. Sci. Pollut. Res. 4, 78–82.

Petzold, A., Schloesser, H., Sheridan, P.J., Arnott, W., Ogren, J.A., Virkkula, A., 2005. Evaluation of multiangle absorption photometry for measuring aerosol light absorption. Aerosol Sci. Technol. 39, 40–51.

Pohjola, M., Pirjola, L., Kukkonen, J., Kulmala, M., 2003. Modelling of the influence of aerosol processes for the dispersion of vehicular exhaust plumes in street environment. Atmos. Environ. 37, 339–351.

Rohr, A.C., Wyzga, R.E., 2012. Attributing health effects to individual particulate matter constituents. Atmos. Environ. 62, 130–152.

Segura, S., Estellés, V., Titos, G., Lyamani, H., Utrillas, M.P., Zotter, P., Prévôt, A.S.H., Močnik, G., Alados-Arboledas, L., Martínez-Lozano, J.A., 2014. Determination and analysis of in situ spectral aerosol optical properties by a multi-instrumental approach. Atmos. Meas. Tech. 7, 2373–2387.

Shah, A.P., Pietropaoli, A.P., Frasier, L.M., Speers, D.M., Chalupa, D.C., Delehanty, J.M., et al., 2008. Effect of inhaled carbon ultrafine particles on reactive hyperemia in healthy human subjects. Environ. Health Perspect. 116, 375–380.

Smit, R., Ntziachristos, L., Boulter, P., 2010. Validation of road vehicle and traffic emission models e a review and meta-analysis. Atmos. Environ. 44, 2943–2953.

Targino, A.C., Krecl, P., Johansson, C., Swietlicki, E., Massling, A., Coraiola, G.C., Lihavainen, H., 2013. Deterioration of air quality across Sweden due to transboundary agricultural burning emissions. Boreal Environ. Res. 18, 19–36.

Transport & Environment, 2016. Dieselgate: Who? what? How? https://www.transportenvironment.org/publications/dieselgate-who-what-how.

Tunved, P., Ström, J., Hansson, H.-C., 2004. An investigation of processes controlling the evolution of the boundary layer aerosol size distribution properties at the Swedish background station Aspvreten. Atmos. Chem. Phys. 4, 2581–2592.

Virkkula, A., Mäkelä, T., Hillamo, R., Yli-Tuomi, T., Hirsikko, A., Hämeri, K., Koponen, I.K., 2007. A simple procedure for correcting loading effects of aethalometer data. J. Air Waste Manag. 57, 1214–1222.

Vouitsis, I., Ntziachristos, L., Samaras, Z., 2013. Methodology for the Quantification of Road Transport PM Emissions, Using Emission Factors or Profiles. TRANSPHORM report, Deliverable D1.1.3. http://www.transphorm.eu/Portals/51/Documents/Deliverables/New%20Deliverables/D1.1.3.pdf.

VTI, 2006. Utvärdering Av Stockholmsför-sökets Effekter På Vägtrafikens Avgasemissioner. (Evaluation of the Stockholm Congestion Tax Effects on Road Traffic Exhaust Emissions) (In Swedish Only). VTI Report 2006-09-19. http://vti.se/en/.

Vu, T.V., Delgado-Saborit, J.M., Harrison, R.M., 2015. Review: Particle number size distributions from seven major sources and implications for source apportionment studies. Atmos. Environ. 122, 114–132.

Wang, D., Liu, Z.C., Tian, J., Liu, J.W., Zhang, J.R., 2012. Investigation of particle emission characteristics from a diesel engine with a diesel particulate filter for alternative fuels. Int. J. Automot. Technol. 13, 1023–1032.

Wang, F., Ketzel, M., Ellermann, T., Wahlin, P., Jensen, S.S., Fang, D., Massling, A., 2010. Particle number, particle mass and NOx emission factors at a highway and an urban street in Copenhagen. Atmos. Chem. Phys. 10, 2745–2764.

Wiedensohler, A., 1988. An approximation of the bipolar charge distribution for

particles in the submicron size range. J. Aerosol Sci. 19, 387–389.

Wiedensohler, A., Birmili, W., Nowak, A., Sonntag, A., Weinhold, K., Merkel, M., Wehner, B., Tuch, T., Pfeifer, S., Fiebig, M., Fjäraa, A.M., Asmi, E., Sellegri, K., Depuy, R., Venzac, H., Villani, P., Laj, P., Aalto, P., Ogren, J.A., Swietlicki, E., Williams, P., Roldin, P., Quincey, P., Hüglin, C., Fierz-Schmidhauser, R., Gysel, M., Weingartner, E., Riccobono, F., Santos, S., Grüning, C., Faloon, K., Beddows, D., Harrison, R., Monahan, C., Jennings, S.G., O'Dowd, C.D., Marinoni, A., Horn, H.-G., Keck, L., Jiang, J., Scheckman, J., McMurry, P.H., Deng, Z., Zhao, C.S., Moerman, M., Henzing, B., de Leeuw, G., Löschau, G., Bastian, S., 2012. Mobility particle size spectrometers: harmonization of technical standards and data structure to facilitate high quality long-term observations of atmospheric particle number size distributions. Atmos. Meas. Tech. 5, 657–685.

WHO, 2016. Ambient Air Pollution: a Global Assessment of Exposure and Burden of Disease. ISBN 9789241511353.

Zhang, K.M., Wexler, A.S., Zhu, Y.F., Hinds, W.C., Sioutas, C., 2004. Evolution of particle number distribution near roadways. Part II: the "Road-to-Ambient" process. Atmos. Environ. 38, 6655–6665.

Zhang, Y., Wang, X., Li, G., Yang, W., Huang, Z., Zhang, Z., Huang, X., Deng, W., Liu, T., Huang, Z., Zhang, Z., 2015. Emission factors of fine particles, carbonaceous aerosols and traces gases from road vehicles: Recent tests in an urban tunnel in the Pearl River Delta, China. Atmos. Environ. 122, 876–884.